

Magnetic and Spectroscopic Properties of LiAuSn

Zhiyun Wu^a, Hellmut Eckert^b, Bernd D. Mosel^b, Manfred H. Möller^a, and Rainer Pöttgen^a

^a Institut für Anorganische und Analytische Chemie und Sonderforschungsbereich 458, Westfälische Wilhelms-Universität Münster, Wilhelm-Klemm-Straße 8, D-48149 Münster, Germany

^b Institut für Physikalische Chemie und Sonderforschungsbereich 458, Westfälische Wilhelms-Universität Münster, Schloßplatz 4/7, D-48149 Münster, Germany

Reprint requests to R. Pöttgen. E-mail: pottgen@uni-muenster.de

Z. Naturforsch. **58b**, 501 – 504 (2003); received February 14, 2003

The stannide LiAuSn was synthesized by reaction of the elements in a sealed tantalum tube. Magnetic susceptibility measurements reveal Pauli paramagnetism. LiAuSn shows a single ¹¹⁹Sn Mössbauer signal at an isomer shift of 2.12(3) mm/s subject to a quadrupole splitting of 1.51(2) mm/s. The ¹¹⁹Sn MAS NMR spectrum reveals a strong Knight shift of 5183 ppm. The unique lithium site present in the crystal structure is reflected by a single ⁷Li NMR signal at 9.8 ppm. While a significant shift of this resonance towards larger frequencies at higher temperature indicates that the *s*-spin density at the lithium sites increases with increasing temperatures, no motional narrowing occurs up to 470 K. This result indicates that the lithium ions are immobile on the NMR timescale within the temperature range observed.

Key words: Stannide, Solid State NMR, Mössbauer Spectroscopy

Introduction

Lithium aluminides, stannides and antimonides are promising candidates as alloy electrode materials for battery applications [1]. The binary compounds have a great advantage when compared with elemental lithium, since the dendrite and whisker growth during the electrodeposition process is significantly reduced. Furthermore, the higher melting points of the binary compounds are favourable. However these intermetallics also have two disadvantages: (i) due to the alloying elements the density increases and (ii) the lithium activity decreases.

In contrast to the detailed phase analytical and electrochemical studies on the binary Li–Al, Li–Sn, and Li–Sb systems [1, and ref. therein], little is known on the structure and properties of ternary compounds. We have recently started a systematic investigation of ternary lithium-transition metal-tin systems with respect to phase analyses, crystal structures, and lithium mobility [2–5]. The structures of a series of new stannides, *i.e.* LiAuSn, LiAu₃Sn₄ [2], LiT₂Sn₄ (*T* = Ru, Rh, Ir) [3], LiPd₂Sn₆, LiRh₃Sn₅, and LiCoSn₆ [4] have been determined. Variable temperature static ⁷Li solid state NMR spectroscopy has proven valuable as a fast-screening method to probe the cationic mobility of lithium in these materials. For example the LiT₂Sn₄

stannides show more or less temperature-independent lineshapes indicating that the ion dynamics in these compounds are rather slow and restricted [5]. This is also the case for LiAuSn. The magnetic and spectroscopic properties of the latter stannide are reported herein.

Experimental Section

Synthesis and X-ray powder diffraction

Starting materials for the preparation of LiAuSn were lithium rods (Merck, > 99%), gold wire (Degussa-Hüls, Ø 1 mm, > 99.9%) and a tin bar (Heraeus, 99.9%). The lithium rods were cut into smaller pieces under dry paraffin oil and subsequently washed with *n*-hexane. The paraffin oil and *n*-hexane were dried over sodium wire. The lithium pieces were kept in Schlenk tubes under argon prior to the reactions. Argon was purified over titanium sponge (900 K), silica gel and molecular sieves.

The lithium pieces were mixed with the gold wire and pieces of the tin bar in the ideal 1:1:1 atomic ratio and sealed in a small tantalum tube under an argon pressure of about 800 mbar in an arc-melting apparatus [6]. The tantalum tube was subsequently enclosed in an evacuated silica tube and first rapidly heated to 1070 K, cooled to 870 K within 3 h, held at this temperature for 2 d, and finally quenched in air by radiative heat loss. The sample could readily be separated from the tube. No reaction with the container material

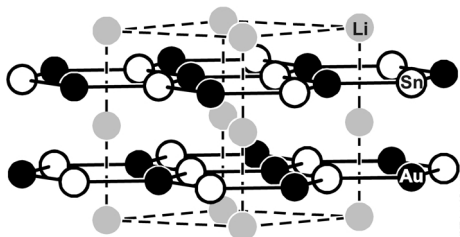


Fig. 1. The crystal structure of hexagonal LiAuSn (space group $P6_3/mmc$). The two-dimensional [AuSn] network is emphasized.

was observed. The light grey polycrystalline sample of LiAuSn is stable in moist air over several weeks.

The purity of the sample was checked through its Guinier powder pattern using $\text{Cu-K}\alpha_1$ radiation and α -quartz ($a = 491.30$ pm, $c = 540.46$ pm) as an internal standard. The experimental pattern was compared with a simulated one [7] using the atomic positions of the structure refinement [2]. The refined hexagonal lattice parameters were in excellent agreement with the previous results.

^{119}Sn Mössbauer spectroscopy

A $\text{Ca}^{119\text{m}}\text{SnO}_3$ source was available for the ^{119}Sn Mössbauer spectroscopic investigation and a palladium foil of 0.05 mm thickness was used to reduce the tin K X-rays concurrently emitted by this source. The measurements were performed in the usual transmission geometry in a commercial helium bath cryostat. The temperature of the absorber was held at 77 K. The source was kept at room temperature in all experiments. The sample was placed within a thin-walled PVC container at a thickness between 10 and 15 mg Sn/cm².

Solid state NMR

^7Li and ^{119}Sn solid state NMR measurements were obtained at 155.5 and 149.8 MHz, respectively, on a Bruker DSX 400 spectrometer equipped with a 4 mm MAS-NMR probe. To avoid excessive heating of these metallic-conducting samples by fast spinning (typically 8 kHz) in the magnetic field, the ground powders were mixed with silica. 90° pulses of 1.8 and 1.5 μs length and relaxation delays of 10 s and 0.5 s were used to record the ^7Li NMR and ^{119}Sn NMR spectra, respectively. Chemical shifts are given in ppm vs. external samples of tetractyltin and a 1 M aqueous solution of LiCl.

Results and Discussion

Crystal chemistry

LiAuSn (Fig. 1) crystallizes with the ZrBeSi type structure, a superstructure of the well known AlB_2 type. The gold and tin atoms are ordered on the boron sites. The $[\text{Au}_3\text{Sn}_3]$ layers are rotated by 60° around

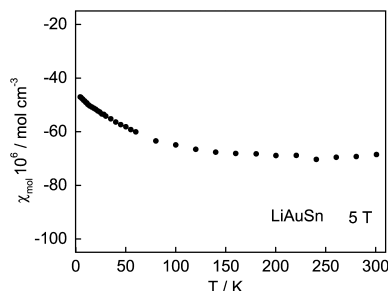


Fig. 2. Temperature-dependence of the magnetic susceptibility of LiAuSn, measured at an external field of 5 T.

the c axis in every other layer, leading to a doubling of the c axis with respect to the AlB_2 type. Within these layers, the Au–Sn distances of 270 pm are slightly smaller than the sum of covalent radii [8] of 274 pm, indicating significant Au–Sn interactions. The layers are well separated from each other by the lithium atoms. Thus, each gold atom has three nearest tin neighbours at 270 pm and two further tin contacts at 302 pm. Electronic structure calculations revealed four times stronger equatorial Au–Sn bonds when compared with the axial ones. Also no distinct Au–Sn bonding is discernible between the hexagonal $[\text{Au}_3\text{Sn}_3]$ layers in the charge density [2]. This result emphasizes the layered, two-dimensional character of LiAuSn from the electronic structure viewpoint.

The lithium atoms are sandwiched by two $[\text{Au}_3\text{Sn}_3]$ hexagons. The Li–Au and Li–Sn distances of 309 pm are both significantly longer than the sums of the covalent radii (256 pm Li+Au and 262 pm Li+Sn) [8]. We can thus assume strong Au–Sn bonding within the layers but weaker bonding of the lithium atoms to these layers. Considering the electropositive lithium atoms and the two-dimensional character of the gold-tin network, electron counting is consistent with the formulation $\text{Li}^{\delta+}[\text{AuSn}]^{\delta-}$.

Magnetism, ^{119}Sn NMR and ^{119}Sn Mössbauer spectroscopy

The temperature dependence of the magnetic susceptibility of LiAuSn is presented in Fig. 2. Over the whole temperature range the susceptibilities are negative. At first sight one might conclude that LiAuSn is a diamagnet. This assumption, however, is in contrast to the metallic behaviour that is evident from the electronic structure calculations. According to the small density-of-states at the Fermi level, we expect a very small Pauli contribution of the conduction electrons to

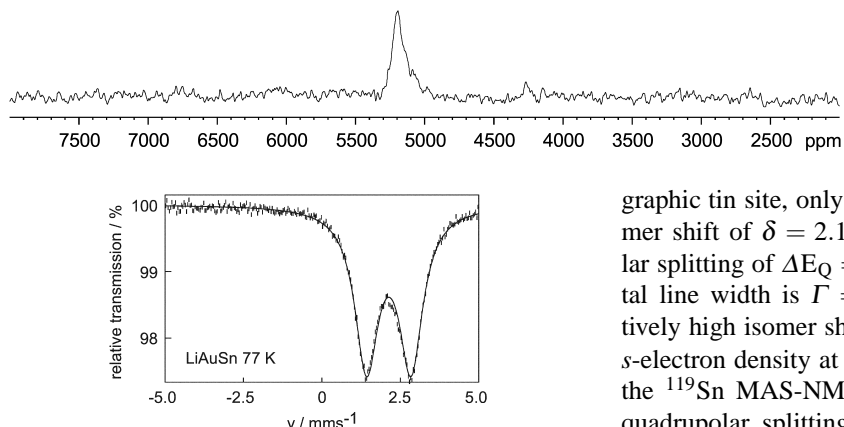


Fig. 4. Experimental and simulated ^{119}Sn Mössbauer spectrum of LiAuSn at 77 K.

the total susceptibility. The large core diamagnetism (mainly contributed from the tin atoms) has a larger absolute value than the Pauli contribution, resulting in negative total susceptibilities over the whole temperature range. This behavior is very similar to that of LiTsn_4 ($T = \text{Ru, Rh, Ir}$) [5].

Fig. 3 shows the ^{119}Sn MAS-NMR spectrum. The ^{119}Sn Knight shift of 5183 ppm is significantly larger than that previously observed by us for a series of LiTsn_4 compounds. The linewidth of 17 KHz is considerable, suggesting a wide distribution of Knight shifts, which may indicate static and/or electronic disordering in the crystal structure. Similarly wide Knight shift distributions have been observed for LiRhSn_4 and LiIrSn_4 , but not for LiRuSn_4 .

The ^{119}Sn Mössbauer spectrum is shown in Fig. 4. In agreement with the existence of a single crystallo-

Fig. 3. ^{119}Sn MAS-NMR spectrum of LiAuSn at room temperature.

graphic tin site, only one signal is observed at an isomer shift of $\delta = 2.12(3)$ mm/s subject to quadrupolar splitting of $\Delta E_Q = 1.51(2)$ mm/s. The experimental line width is $\Gamma = 0.91(3)$ mm/s. From the relatively high isomer shift we can infer a relatively high s -electron density at the tin atoms, in agreement with the ^{119}Sn MAS-NMR result. The high value of the quadrupolar splitting parameter reflects a relatively strong deviation from cubic symmetry. An even larger quadrupole splitting parameter of $\Delta E_Q = 1.98(2)$ mm/s was observed for CeRu_4Sn_6 [9]. Within the temperature interval $4\text{ K} < T < 300\text{ K}$ the lineshape of the spectra remains unchanged.

^7Li Solid state NMR

Fig. 5 shows the ^7Li MAS NMR spectrum at room temperature. The observation of a single resonance is consistent with the existence of one unique lithium site as revealed by the single crystal diffraction data. The resonance shift of 9.8 ppm reflects a low s density of states and dominating ionic character of lithium binding, consistent with the formulation as $\text{Li}^{\delta+}[\text{AuSn}]^{\delta-}$. Weak spinning sidebands arise from the first order quadrupolar shifted outer Zeeman transitions. At elevated temperatures, the ^7Li resonance shifts to significantly more positive values, suggesting that the s -spin density at the Fermi level localized at the lithium sites

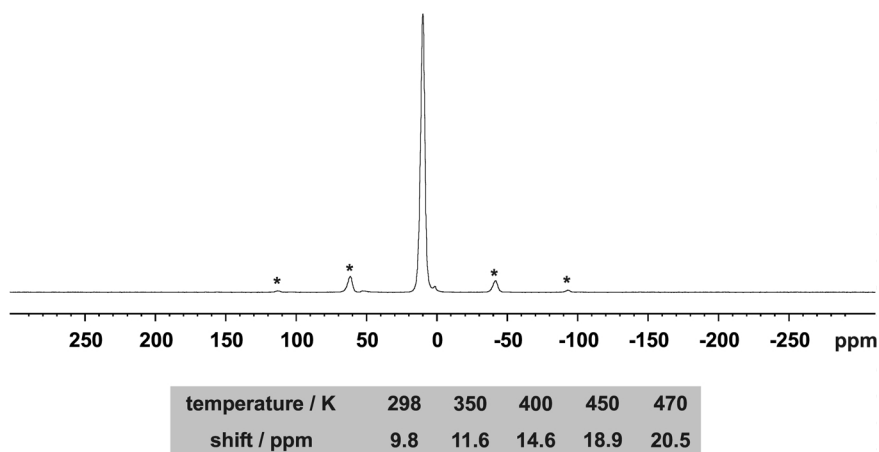


Fig. 5. ^7Li MAS NMR spectrum in LiAuSn at room temperature; MAS spinning sidebands (spinning speed 8 kHz) are marked by asterisks. ^7Li shifts at elevated temperatures are listed below.

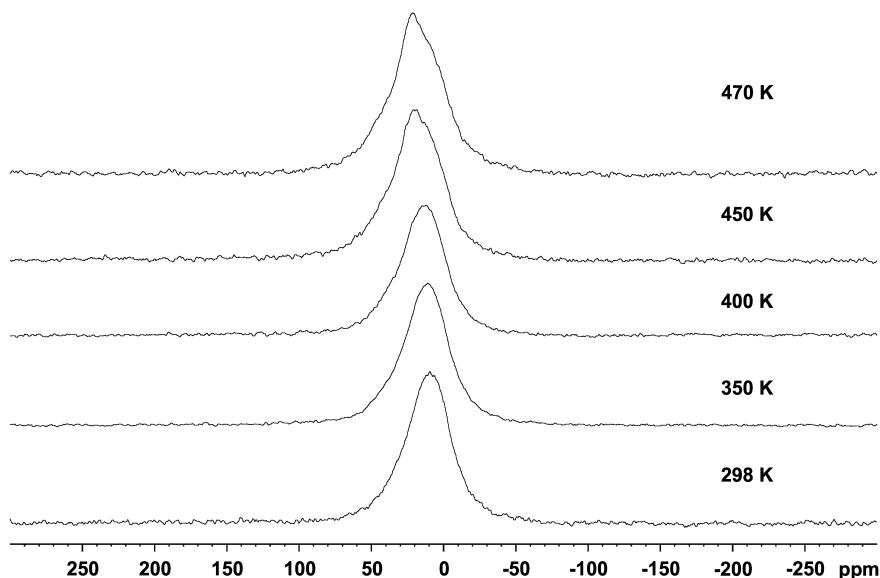


Fig. 6. Static ^7Li NMR spectra between 298 and 470 K. Note the absence of motional narrowing effects.

increases significantly with temperature. A similar effect was previously observed in LiTsn_4 ($T = \text{Rh, Ir}$) compounds [5].

To detect a potential cationic mobility of lithium, we also recorded the temperature dependence of ^7Li static spectra in LiAuSn between 300 K and 470 K (see Fig. 6). At room temperature the static linewidth is 5.6 kHz. The dominant contribution to this value arises from the ^7Li - ^7Li homonuclear dipole-dipole coupling, which amounts to 4.0 kHz, as calculated from the van Vleck formula. The excess linewidth probably arises from the effect of the ^7Li Knight shift anisotropy. If lithium ion diffusion were activated on the ms timescale, the static broadening should be suc-

cessively reduced, leading to a significant linewidth decrease with increasing temperature. Our result reveals the absence of such a “motional narrowing” effect up to 470 K. The low lithium mobility in LiAuSn detected in our studies is consistent with the crystal structure, which shows that (i) the lithium site is fully occupied, and (ii) there are no accessible interstitial sites to maintain cation transport.

Acknowledgements

We thank the Degussa-Hüls AG for a generous gift of gold wire. This work was financially supported by the Fonds der Chemischen Industrie and by the Deutsche Forschungsgemeinschaft through SFB 458 *Ionenbewegung in Materialien mit ungeordneten Strukturen*.

- [1] R. A. Huggins, Lithium Alloy Electrodes, in: J. O. Besenhard (ed.) *Handbook of Battery Materials*, Wiley-VCH, Weinheim (1999).
- [2] R.-D. Hoffmann, D. Johrendt, Zh. Wu, R. Pöttgen, *J. Mater. Chem.* **12**, 676 (2002).
- [3] Zh. Wu, R.-D. Hoffmann, R. Pöttgen, *Z. Anorg. Allg. Chem.* **628**, 1484 (2002).
- [4] R. Pöttgen, Zh. Wu, R.-D. Hoffmann, G. Kotzyba, H. Trill, J. Senker, D. Johrendt, B. D. Mosel, H. Eckert, *Heteroatom Chem.* **13**, 506 (2002).
- [5] Zh. Wu, H. Eckert, J. Senker, D. Johrendt, G. Kotzyba, B. D. Mosel, H. Trill, R.-D. Hoffmann, R. Pöttgen, *J. Phys. Chem. B* **107**, 1943 (2003).
- [6] R. Pöttgen, Th. Gulden, A. Simon, *GIT-Laborfachzeitschrift* **43**, 133 (1999).
- [7] K. Yvon, W. Jeitschko, E. Parthé, *J. Appl. Crystallogr.* **10**, 73 (1977).
- [8] J. Emsley, *The Elements*, 3rd edn, Oxford University Press, Oxford (1999).
- [9] R. Pöttgen, R.-D. Hoffmann, E. V. Sampathkumaran, I. Das, B. D. Mosel, R. Müllmann, *J. Solid State Chem.* **134**, 326 (1997).